Exact zeros of entanglement for arbitrary rank-two mixtures derived from a geometric view of the zero polytope

Andreas Osterloh*
Institut für Theoretische Physik, Universität Duisburg-Essen, D-47048 Duisburg, Germany
(Received 29 September 2016; published 23 December 2016)

Here I present a method for how intersections of a certain density matrix of rank 2 with the zero polytope can be calculated exactly. This is a purely geometrical procedure which thereby is applicable to obtaining the zeros of SL- and SU-invariant entanglement measures of arbitrary polynomial degree. I explain this method in detail for a recently unsolved problem. In particular, I show how a three-dimensional view, namely, in terms of the Bloch-sphere analogy, solves this problem immediately. To this end, I determine the zero polytope of the three-tangle, which is an exact result up to computer accuracy, and calculate upper bounds to its convex roof which are below the linearized upper bound. The zeros of the three-tangle (in this case) induced by the zero polytope (zero simplex) are exact values. I apply this procedure to a superposition of the four-qubit Greenberger-Horne-Zeilinger and W state. It can, however, be applied to every case one has under consideration, including an arbitrary polynomial convex-roof measure of entanglement and for arbitrary local dimension.

DOI: 10.1103/PhysRevA.94.062333

I. INTRODUCTION

Entanglement is one of the key features of quantum mechanics that is omnipresent in mutually interacting systems. Measures of entanglement are minimally invariant under local unitaries [1]. This invariance emerges when dealing with the concept of local operations combined with classical communication (LOCC). It has, however, soon been realized that this invariance group has to be extended to the special linear group [2–4] since in general stochastic local operations combined with classical communication (SLOCC) have to be included. Thus, a state $|\psi\rangle$ is said to be equivalent to the state $|\psi'\rangle := (A_1 \otimes \cdots \otimes A_q)|\psi\rangle$ for $A_i \in \mathrm{SL}(d_i)$, and for each SL-invariant measure τ of entanglement we have $\tau(|\psi\rangle) = \tau(|\psi'\rangle)$. Every such SL-invariant entanglement measure can be decomposed into polynomial measures of entanglement of homogeneous degree.

The entanglement content of a mixed state is represented by the convex-roof expression of the entanglement measure of interest [1]. Whereas it is more easy to write the convex roof down than to really calculate it, it has shown to be an exactly solvable task for measures, which are SL-invariant homogeneous polynomials of rank 2, as the concurrence [5,6], respectively, convex functions of them. In this simple case, the optimal decomposition has a continuous degeneracy, which is a key ingredient to the exact solution. However, already if the homogeneous degree is four, this degeneracy is lost in general and one is left with a typically unique solution in terms of normalized states, not considering global phases and permutations of the states. It has therefore become one of the central problems in modern physics to "tame" the convex roof [7]. First steps into this direction have been taken in [8–10] where lower bounds for rank-2 density matrices have been addressed with some thoughts about the more general case [10]. In some specific cases this lower bound coincides with the convex-roof solution. With these solutions, certain particular cases for rank-3 density matrices [11] and even higher rank [12], which are all constructions out of separable states, have followed.

The convexified minimal *characteristic curve* [8–10] of the entanglement measure under consideration has been singled out as a lower bound to any possible decomposition of ρ. This has been advanced to calculate lower bounds to the three-tangle of density matrices with general rank [13–15], a lower bound which was shown to be sharp for the class of states with the symmetry of the Greenberger-Horne-Zeilinger (GHZ) state, termed *GHZ symmetry*. This technique for obtaining lower bounds has served later for demonstrating bound entanglement with positive partial transpose for qutrit states [16].

In the meantime several algorithms providing upper bounds emerged [17–19], where [19] is departing from the solution for the zero polytope for rank-2 density matrices. However, also applications of the original method provided in [8–10] are still challenging [20,21]. In their recent contribution, Jung and Park [21] have tempted to test the monogamy relations of Coffman, Kundu, and Wootters (CKW) [22] and for the negativity [23,24] towards possible extended versions [25–28]. They succeeded for the negativity, however they encountered problems for the Coffman-Kundu-Wootters monogamy, which they highlighted using a toy example in their appendix. The main difference to the case depicted in [8] was that no three zeros of the three-tangle coincided for a given probability $p \in [0,1]$. Hence their characteristic curves had zeros at three different probabilities. There, the case of noncoinciding zeros of the characteristic curves was posed as an open problem.

We first focus on their toy example since it shows (1) how using $C_3 := \sqrt{|\tau_3|}$ instead of $|\tau_3|$ can help in calculating meaningful upper bounds of its convex roof and (2) the impact noncoinciding roots have on the three-tangle of the state under consideration. The intervals where the mixed three-tangle is zero can be obtained in a simple geometrical way: they are numerically exact results.

This work is outlined as follows. In the next section, I briefly focus on the method and give as an example the three-tangle as SL-invariant homogeneous polynomial of degree 4 with reference to [21]. Next, I apply this method to the toy example of [21] in Sec. IV and come to some general states in Sec. V. I

*andreas.osterloh@uni-due.de

briefly comment on extended monogamy relations in Sec. VI before making concluding remarks in Sec. VII.

II. PRELIMINARIES

Measures of entanglement are minimally invariant under local unitaries $\prod_{i=1}^{q;\otimes} \mathrm{SU}(d_i)$[1] where q is the number of local objects of dimension d_i , $i = 1, \ldots, q$ which are being considered. Hence, all states $|\psi'\rangle := (U_1 \otimes \cdots \otimes U_q)|\psi\rangle$ with $U_i \in \mathrm{SU}(d_i)$ are considered equivalent. An SU-invariant measure of entanglement $\mathcal{M}$ satisfies

$$\mathcal{M}(|\psi'\rangle) = \mathcal{M}(|\psi\rangle). \tag{1}$$

This invariance is connected to LOCC. It has, however, been realized that this invariance group has to be extended to the special linear version $\prod_{i=1}^{q;\otimes} \mathrm{SL}(d_i)$[2–4] since in general SLOCC must be considered. There, a state $|\psi\rangle$ is said to be equivalent to the state $|\psi'\rangle := (A_1 \otimes \cdots \otimes A_q)|\psi\rangle$ for $A_i \in \mathrm{SL}(d_i)$, and for each SL-invariant measure τ of entanglement holds

$$\tau(|\psi\rangle) = \tau(|\psi'\rangle). \tag{2}$$

Every SL-invariant entanglement measure can be decomposed into polynomial measures of entanglement of homogeneous degree. I will for brevity write $\tau(\psi)$ for $\tau(|\psi\rangle)$.

It is, however, remarked that the entanglement content in the state is nevertheless modified in that the modulus $\langle\psi|\psi\rangle$ is modified in general by SL operations in contrast to the SU invariance.

I will consider $C_3 := \sqrt{|\tau_3|}$ as entanglement measures, where the three-tangle $|\tau_3|$ has been defined as [22] (see also [29–31])

$$\begin{aligned}
\tau_3 &= d_1 - 2d_2 + 4d_3,\\
d_1 &= \psi_{000}^2\psi_{111}^2 + \psi_{001}^2\psi_{110}^2 + \psi_{010}^2\psi_{101}^2 + \psi_{100}^2\psi_{011}^2,\\
d_2 &= \psi_{000}\psi_{111}\psi_{011}\psi_{100} + \psi_{000}\psi_{111}\psi_{101}\psi_{010}\\
&\quad + \psi_{000}\psi_{111}\psi_{110}\psi_{001} + \psi_{011}\psi_{100}\psi_{101}\psi_{010}\\
&\quad + \psi_{011}\psi_{100}\psi_{110}\psi_{001} + \psi_{101}\psi_{010}\psi_{110}\psi_{001},\\
d_3 &= \psi_{000}\psi_{110}\psi_{101}\psi_{011} + \psi_{111}\psi_{001}\psi_{010}\psi_{100}
\end{aligned}$$

and coincides with the three-qubit hyperdeterminant [32,33]. It is the only continuous SL invariant here, meaning that every other such SL invariant for three qubits can be expressed as a function of τ_3.

III. GEOMETRIC VIEW OF THE ZERO POLYTOPE

For rank-2 density matrices ρ, the states in the range of ρ can be written as

$$|\psi(z)\rangle := |\psi_1\rangle + z|\psi_2\rangle, \tag{3}$$

with eigenstates $|\psi_i\rangle$ of ρ, and $z \in \mathbb{C}$ [10]. An entanglement measure τ vanishes precisely on the polytope with the states $|\psi(z_0)\rangle$ as vertices, where $z_0 \in \mathbb{C}$ satisfies the equation $\tau(\psi(z_0)) = 0$; this object is called the *zero polytope* [8,10] (see also [20]). One can hence check what triangle between vertices of the zero polytope has an intersection with the line connecting $|\psi_1\rangle$ with $|\psi_2\rangle$ at some $p_{0;i}$ for $i \in \mathcal{I}$. The values $p_{\mathrm{low}} = \min_{i\in\mathcal{I}} p_{0;i}$ and $p_{\mathrm{high}} = \max_{i\in\mathcal{I}} p_{0;i}$ is the interval where $\rho(p) := p|\psi_1\rangle\langle\psi_1| + (1-p)|\psi_2\rangle\langle\psi_2|$ is zero. I have used here a part of the algorithm described in [19] [see Eqs. (10) and (11) therein]. This procedure is illustrated in Fig. 1 where I give an example for a polynomial of (homogeneous) degree 4 on the Bloch sphere.

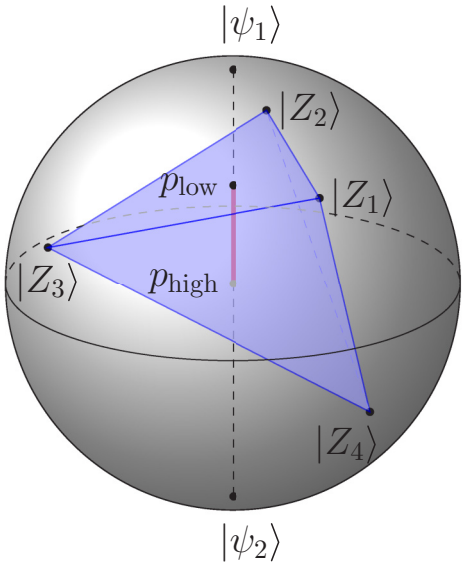

FIG. 1. An example for a (homogeneous) polynomial SL-invariant τ for a density matrix of rank 2; $\rho(p) = p|\psi_1\rangle\langle\psi_1| + (1-p)|\psi_2\rangle\langle\psi_2|$ is drawn in the Bloch sphere picture. The polynomial invariant has the four solutions $|Z_i\rangle$ for $i \in \{1, \ldots, 4\}$ defining the zero polytope. The intersection of this polytope with the line connecting $|\psi_1\rangle$ and $|\psi_2\rangle$ leads to an interval $[p_{\mathrm{low}}, p_{\mathrm{high}}]$ of vanishing $\tau[\rho(p)]$. When this intersection is empty, this means that $\rho(p)$ is always entangled as measured by τ.

For density matrices of higher rank R, the states in the range of ρ can be written as

$$|\psi(z_1, \ldots, z_{R-1})\rangle := |\psi_1\rangle + z_1|\psi_2\rangle + \cdots + z_{R-1}|\psi_R\rangle, \tag{4}$$

and the zero polytope turns into the convexification of the *zero manifold* made out of all the solutions of $\tau[\psi(z_{0;1}, \ldots, z_{0;R-1})] = 0$.

IV. THE TOY EXAMPLE RAISED BY JUNG AND PARK

To show this method at work, I choose the toy example out of the appendix of [21].

A. The geometric view

We define the n-qubit GHZ and W states as

$$|\mathrm{GHZ}_n\rangle = \frac{1}{\sqrt{2}}(|00\ldots0\rangle + |11\ldots1\rangle), \tag{5}$$

$$|W_n\rangle = \frac{1}{\sqrt{3}}(|0\ldots01\rangle + |0\ldots10\rangle + \cdots + |10\ldots0\rangle) \tag{6}$$

where we consider the three-qubit example first,

$$|\mathrm{GHZ}_3\rangle = \frac{1}{\sqrt{2}}(|000\rangle + |111\rangle), \tag{7}$$

$$|W_3\rangle = \frac{1}{\sqrt{3}}(|001\rangle + |010\rangle + |100\rangle), \tag{8}$$

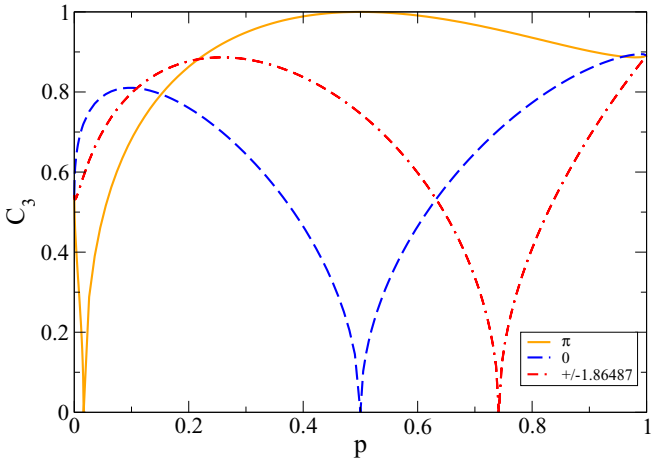

FIG. 2. I show here the four characteristic curves for C_3 which become zero: two single real zeros at $p \approx 0.01636$ (solid orange curve) and $p = 0.5$ (dashed blue curve) corresponding to an angle $\varphi = \pi$ and 0, respectively, and the two coinciding curves which are zero at $p \approx 0.7418$ (dash-dash-dotted red curve). The latter curve corresponds to two complex conjugate solutions z_0. Both curves are for the angle $\varphi = \pm 1.8649 = \arg(z_0)$ as shown in the legend. The angles of z for the different curves are shown in the legend.

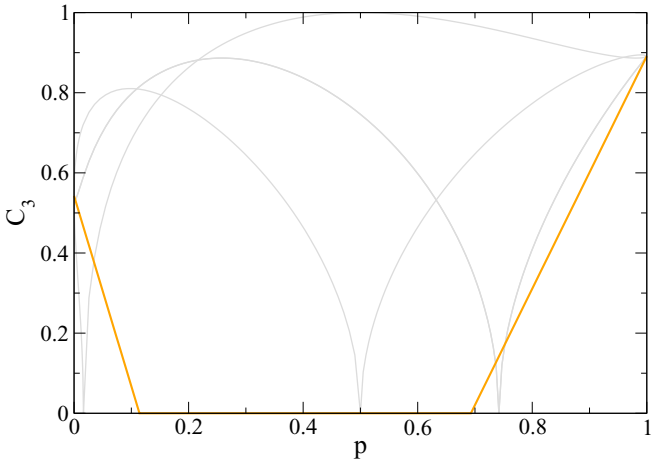

FIG. 3. An upper bound to the convex roof is shown for $\rho(p)$ (orange line). It is piecewise linearly interpolating between $(p, C_3) = (0, \sqrt{8\sqrt{6} - 9}/6)$, (0.11423,0), (0.69289,0), and $(1, \sqrt{8\sqrt{6} + 9}/6)$. The intersection of $\rho(p)$ with the zero simplex of the three-tangle is an exact result, whereas the linear extrapolation is certainly an upper bound to $\widehat{C_3} = \widehat{\sqrt{|\tau_3|}}$; it results from a superposition of the corresponding pure state and the density matrix with zero three-tangle closest to it. Therefore the density matrix would be decomposed into three states for $0 < p < 0.114230$ and into four states for $0.692885 < p < 1$. The characteristic curves are the gray curves in the background; they serve in order to demonstrate how the intersection with the zero simplex, due to its convexity, leads to a shrinking of the region where $\widehat{C_3}[\rho(p)] = 0$.

and the density matrix

$$\rho(p) = p|\psi_+\rangle\langle\psi_+| + (1-p)|\psi_-\rangle\langle\psi_-|, \tag{9}$$

where

$$|\psi_\pm\rangle = \frac{1}{\sqrt{2}}(|\mathrm{GHZ}_3\rangle \pm |W_3\rangle). \tag{10}$$

These states satisfy the orthogonality condition $\langle\psi_+|\psi_-\rangle = 0$. In order to calculate or estimate the three-tangle in $\rho(p)$, we have to consider the characteristic curves [8,10], hence

$$C_3(p,\varphi) := C_3[Z(p,\varphi)] \tag{11}$$

for the states

$$|Z(p,\varphi)\rangle := \sqrt{p}|\psi_+\rangle - e^{i\varphi}\sqrt{1-p}|\psi_-\rangle. \tag{12}$$

Some of them are shown in Fig. 2 (more can be found in [21]). It is hence useful to look for solutions z_0 to the equation

$$\tau_3(|\psi_+\rangle - z|\psi_-\rangle) = 0. \tag{13}$$

The zeros $z_{0;j}$, $j = 1,\ldots,2n$ with $n \in \mathbf{N}$, describe the vertices of a zero polytope, which becomes a three-dimensional zero simplex in this case. I want to emphasize that the zero simplex is an exact result and therefore the values p of $\rho(p)$ which are lying inside the zero simplex are the only values for which the convex roof of $\rho(p)$ vanishes. Hence, it is also clear that the complement is made out of states with nonzero convex roof. The zeros of Eq. (13) are

$$\boldsymbol{z_0} = (z_{0;1}, z_{0;2}, z_{0;3}, z_{0;4}) \tag{14}$$

$$\approx (1, -7.7543, 0.5899e^{1.8649i}, 0.5899e^{-1.8649i}). \tag{15}$$

I want to emphasize that although the values for the zeros are exact, they are nevertheless approximated here since it is cumbersome to write them down analytically; in addition, I do not attribute to the knowledge of the exact values any further insight. With $p_0 = p(z_0) = 1/(1+|z_0|^2)$, hence

$$\boldsymbol{p_0} = (p_{0;1}, p_{0;2}, p_{0;3}, p_{0;4}) \approx (1/2, 0.01636, 0.74182, 0.74182), \tag{16}$$

the values $p_0 z_0$ are those to be convexly combined to zero [19,20]. The result is that for $p \in [0.11423, 0.69289]$ the convex roof of the three-tangle is zero. The decomposition of $\rho(p)$ in $p = 0.11423$ is given by $|Z(p_{0;1},0)\rangle$ with weight 0.202362 and $|Z(p_{0;2},\pi)\rangle$ with weight 0.797638; at $p = 0.692885$ it is given by $|Z(p_{0;1},0)\rangle$ with weight 0.202362 and the states $|Z(p_{0;3} = p_{0;4}, \pm 1.86487)\rangle$ with weights 0.398819 each. It is a curious coincidence that the weight of $|Z(p_{0;1},0)\rangle$ takes about the same value; they deviate only by 3×10^{-16}.

An upper bound to the convex roof $\widehat{C_3}$ is shown in Fig. 3 together with the characteristic (gray background) curves: the upper bound to the convex roof is a piecewise straight (orange) line. I will therefore call it the *linearized* upper bound.

B. Beyond linearization

The strong concavity of the characteristic curves around their zeros, together with the fact that the plotted characteristic curves close to their zeros are a lower bound to other characteristic curves, tells that whatever decomposition vector of the density matrix one will take it will yield a concave result at least in the vicinity of the zero simplex. This modifies close to $p = 0$ or 1 where it is rather likely that a piecewise convex curve might be obtained, in particular in the interval

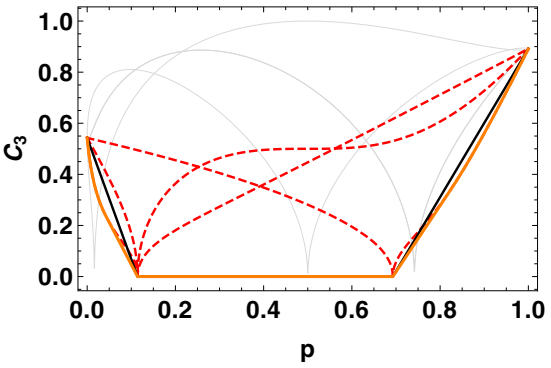

FIG. 4. Here, I show results for some particular decompositions of $\rho(p)$ (see text for details). The characteristic curve with a single zero at $p = 0.01636$, corresponding to an angle $\varphi = \pi$, initially is strictly convex. Therefore those decompositions containing a state $|Z(q,\pi)\rangle$ will be also strictly convex close to the points $p = 0,1$. That this is indeed the case also for p close to 1 is shown by the red dashed curves, which come to lie below the upper linearized bound (thin black line). The corresponding new lower bound is the thick orange line.

[0,0.11423] where one of the characteristic curves is strongly convexly decreasing with a zero at $p \approx 0.01636$. I therefore try for a slightly different decomposition here in order to check whether the convexity of this characteristic curve might lead to a curve which somewhere lies below the straight line. I chose to decompose the matrix $\rho(p)$ into two states, namely, into the state $|Z(p_{0;1},0)\rangle$ and the corresponding state $|Z(q(p,p_{0;1}),\pi)\rangle$ with $q(p,p_{0;1})$ in the interval given by p and $p_{0;1}$ such that the line connecting the states $|Z(p_{0;1},0)\rangle$ and $|Z(q(p,p_{0;1}),\pi)\rangle$ on the Bloch sphere hits the point on the z axis corresponding to $\rho(p)$. A further decomposition I examined is the equal mixture of the two states $|Z(p_{0;3} = p_{0;4}, \pm 1.86487)\rangle$ with $|Z(q(p,p_{0;1}),0)\rangle$ such that the line interconnecting the two states is again passing through $\rho(p)$. The result is shown as red dashed lines in Fig. 4. Some of them are lying below the straight line, demonstrating that a better upper bound than the linearized one is obtained for the convex roof $\widehat{C}_3$. It is linear close to the borders of the interval [0.11423,0.692885] up to $p_r = 0.8240$ and down to $p_l = 0.04395$, showing that the decomposition is made of convex decompositions of the two states $|Z(p_{0;3} = p_{0;4}, \pm 1.86487)\rangle$ and a third state $|Z(q(p_{l/r},p_{0;1}),0)\rangle$ (see [8,10]). Beyond, it is strictly convex, telling that the decomposition is here made of the two states $|Z(p_{0;3} = p_{0;4}, \pm 1.86487)\rangle$ and the state $|Z(q(p,p_{0;1}),0)\rangle$, which depends on p.

This procedure will be repeated for the general rank-2 case in the next section. It can be applied for general rank-2 density matrices and, using the results of [19], also for obtaining useful upper bounds for general rank. It is a purely geometric method and, therefore, it is not restricted to qubits.

V. THE INTERESTING CASE

In order to demonstrate how the combined method of the geometric view on the zero polytope with generalized decompositions eventually going beyond the linearized method of [19] works for the general case, we present the slightly modified example from [21].

A. The geometric view

Thus, we turn to the more general example where the pure state

$$|\Psi_4(p,\varphi)\rangle := \sqrt{p}\,|\mathrm{GHZ}_4\rangle - \sqrt{1-p}e^{i\varphi}\,|W_4\rangle \tag{17}$$

of four qubits was given [21]. It is a permutation invariant state whose three-qubit density matrices, for their permutational symmetries, all have the same form

$$\rho_3(p,\varphi) = q(p)|\psi_1(p,\varphi)\rangle\langle\psi_1(p,\varphi)| + [1-q(p)]|\psi_2(p,\varphi)\rangle\langle\psi_2(p,\varphi)| \tag{18}$$

with $q(p) = \frac{2+\sqrt{1-p^2}}{4}$ and

$$\psi_1(p,\varphi) = f_1(p)e^{i\varphi}|111\rangle + g_1(p)|000\rangle + h_1(p)e^{-i\varphi}|W_3\rangle, \tag{19}$$

$$\psi_2(p,\varphi) = f_2(p)e^{i\varphi}|111\rangle + g_2(p)|000\rangle + h_2(p)e^{-i\varphi}|W_3\rangle. \tag{20}$$

Here, the functions are defined as

$$f_1(p) := \sqrt{\frac{2}{(1+p)(3-p)+(3+p)\sqrt{1-p^2}}}\,p, \tag{21}$$

$$g_1(p) := \sqrt{p\frac{4\sqrt{1-p^2}-3p+5}{(3+p)\sqrt{1-p^2}+(1+p)(3-p)}}, \tag{22}$$

$$h_1(p) := \sqrt{\frac{3p(1-p)}{(1+p)^2-(1-p)\sqrt{1-p^2}}}, \tag{23}$$

$$f_2(p) := \sqrt{\frac{2}{(1+p)(3-p)-(3+p)\sqrt{1-p^2}}}\,p, \tag{24}$$

$$g_2(p) := \sqrt{p\frac{4\sqrt{1-p^2}+3p-5}{(3+p)\sqrt{1-p^2}-(1+p)(3-p)}}, \quad \mathrm{sign}\,(3-5p) \tag{25}$$

$$h_2(p) := -\sqrt{\frac{3p(1-p)}{(1+p)^2+(1-p)\sqrt{1-p^2}}}. \tag{26}$$

The three-tangle is a periodic function of φ with period $\pi/2$, because of the four-qubit permutation symmetry of the state. We show the results of the algorithm from [19], which except the default linearization gives an exact result for the zeros, in Fig. 5. It is an upper bound to $\widehat{C}_3$.

B. Beyond linearization

In order to test whether it is possible also here to come below the linearized upper bound, I checked the zeros of Eq. (13) and the particular decompositions I have described in detail in the last section.

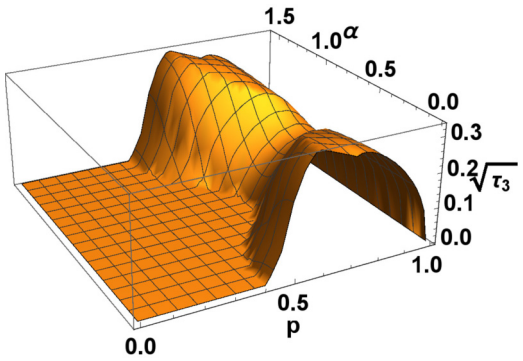

FIG. 5. The upper bound for $\widehat{C_3}$ where one linearizes between the values for the states $|\psi_i(p,\varphi)\rangle$ and the corresponding extreme intersection points $p_{0;i}$, for $i = 1,2$, of the line represented by $\rho(p)$ and the zero simplex.

In $[0.722074,1]$, there are four real solutions. For the remaining values of p, there are two complex conjugate solutions besides two which stay real. One decomposition for which the three-tangle vanishes is always made from real solutions here, whereas the other one is made out of three pure states: one corresponding to a real solution and the two complex conjugate solutions. The zero simplex is varying its dimension as shown in Fig. 6 for $\varphi = 0$ and $\pi/4$, respectively. It is becoming zero twice for $\varphi = 0$: a single point, where the line spanned by the complex conjugate values with nonzero imaginary part crosses the corresponding line between the two other real values, and there is a whole interval $[0.722074,1]$ for p where the zero simplex is two dimensional. There, four real solutions appear. This feature, however, is not stable against small perturbations in φ.

The single zero disappears for $\varphi \gtrsim 0.5236$ with the zero simplex being everywhere three dimensional (except at the boundaries), in particular for $\varphi = \pi/4$. This is indicated in Fig. 7.

An upper bound to the three-tangle $\widehat{C_3}$ is shown in Fig. 8 for $\varphi = 0$ in the linearized version and the procedure described in Sec. IV B (see also the discussion of Fig. 4 in the text). It is seen that both basically coincide close to the zeros but

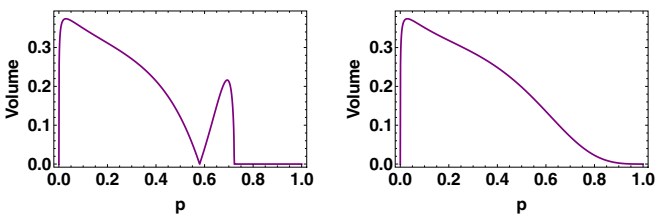

FIG. 6. The volume of the zero simplex for two values of $\varphi = 0$ (left panel) and $\pi/4$ (right panel). For $\varphi = 0$ the volume grows to a finite value for diminishing again unless it is crossing with zero volume (staying, however, two-dimensional) to grow again up to a value of $p = 0.722074$ where it again becomes two dimensional up to $p = 1$. Here, the imaginary part of the two corresponding solutions is zero and we have again four real values. This passage through zero in between is missing for $\varphi = \pi/4$; in particular the zero simplex is always three dimensional for $p \in (0,1)$.

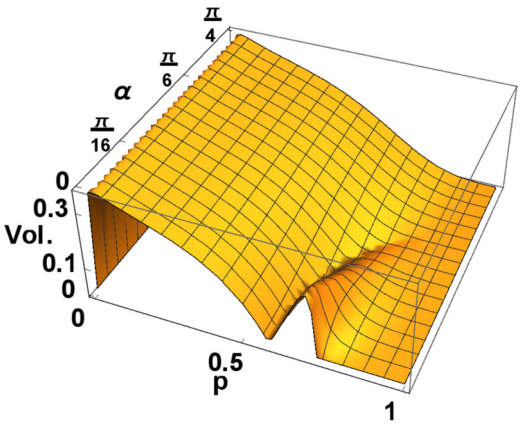

FIG. 7. A three-dimensional plot of the zero-simplex dimension.

they deviate considerably in between. This is not the case for $\varphi = \pi/4$, where both curves coincide (not shown here).

VI. EXTENDED MONOGAMY

It is clear that the residual tangle is not measured in general by an SL-invariant quantity [34]. Therefore it makes little sense to subtract an SL-invariant quantity from the residual tangle, which has no SL-invariance. When nevertheless doing so, one recognizes that the monogamy cannot be extended with the usual three-tangle $\widehat{|\tau_3|}$ or even its square root $\widehat{\sqrt{|\tau_3|}}^2 = \widehat{C_3}^2$ [25–27]. The ultimate possibility would be $\widehat{\sqrt[4]{|\tau_3|}}^4$, which could not be excluded for pure states of four qubits [35]. This does not mean that it will not be excluded for some n-qubit pure state with $n > 4$. This question has to be answered in future work. As far as the extended monogamy relations are concerned, the states already satisfy it if one is considering $\widehat{C_3}^2$ as a measure for the three-tangle. This can be seen in Fig. 9 taking the linearized upper bound for $\widehat{C_3}^2$; it therefore provides a lower

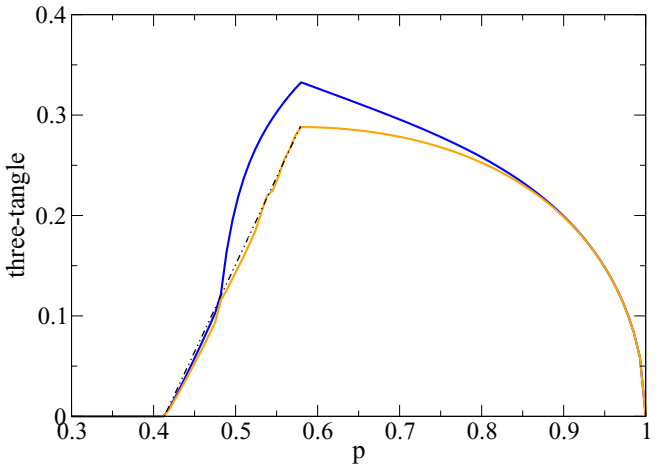

FIG. 8. Two upper bounds for $\widehat{C_3}$ for $\varphi = 0$ as a function of p. Besides the linearized version from [19] (upper blue curve) also the one coming out of the procedure described here (see discussion of Fig. 4) is shown (orange lower curve). This curve is well approximated with the straight black dash-dotted line in the figure. It can be seen, however, that the convex roof lies at least slightly below the straight line.

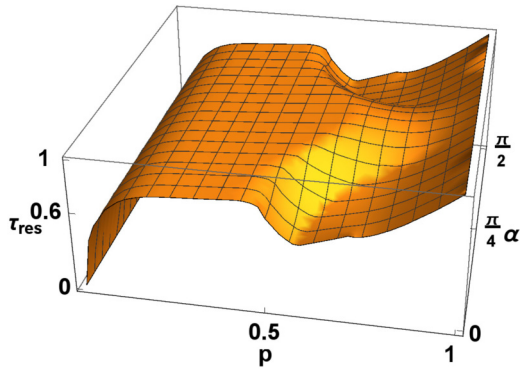

FIG. 9. The extended residual tangle [25–27,35] using $\widehat{C_3}^2$ as the measure for the three-tangle. I do not show the outcome for $\sqrt{\widehat{C_3}^4}$, since it is smaller than $\widehat{C_3}^2$ [20] and accordingly the residual tangle is bigger.

bound for the residual "four-tangle". It is ranging from zero (for the W states) to one (for the GHZ states).

VII. CONCLUSIONS

I have presented a method for how intersections of a certain density matrix of rank 2 with the zero polytope can be calculated exactly. This is an exact solution to every problem of noncoinciding zeros of the zero polytope, as inserted in the algorithm of [19]. I have exemplified this method on an open problem recently raised by Jung and Park [21]. I have described in detail for the toy example of [21] how the simplest linearized version of an upper bound can be obtained, and how one can go beyond it. To this end, I calculate a meaningful upper bound of the three-tangle $C_3 = \sqrt{|\tau_3|}$ for their toy example which is better than the linear interpolation in [19]. As a proof of principles, I apply this formalism further to the general case of superpositions of four-particle GHZ and W states, calculating the linearized form for the upper bound together with the extended version for C_3. As a byproduct I briefly comment on the extended CKW monogamy and provide a graph also for a generalized four-tangle. I want to mention that the calculation of the three-tangle of $\rho = p|\mathrm{GHZ}_4\rangle\langle\mathrm{GHZ}_4| + (1-p)|W_4\rangle\langle W_4|$ is trivially zero for each three-qubit subsystem.

As a purely geometrical procedure the findings of this work are applicable to obtaining the zeros of general SL- and also of arbitrary SU-invariant polynomial entanglement measures with bidegree (d_1,d_2) [36,37]; this holds as well for the procedure of going beyond the linear interpolation. They are also applicable to qudits. The same line of thought can be adopted for arbitrary rank density matrices [19].

ACKNOWLEDGMENT

I acknowledge discussions with K. Krutitsky and R. Schützhold.

[1] G. Vidal, J. Mod. Opt. **47**, 355 (2000).
[2] W. Dür, G. Vidal, and J. I. Cirac, Phys. Rev. A **62**, 062314 (2000).
[3] F. Verstraete, J. Dehaene, and B. De Moor, Phys. Rev. A **65**, 032308 (2002).
[4] F. Verstraete, J. Dehaene, B. De Moor, and H. Verschelde, Phys. Rev. A **65**, 052112 (2002).
[5] W. K. Wootters, Phys. Rev. Lett. **80**, 2245 (1998).
[6] A. Uhlmann, Phys. Rev. A **62**, 032307 (2000).
[7] B. Jungnitsch, T. Moroder, and O. Gühne, Phys. Rev. Lett. **106**, 190502 (2011).
[8] R. Lohmayer, A. Osterloh, J. Siewert, and A. Uhlmann, Phys. Rev. Lett. **97**, 260502 (2006).
[9] C. Eltschka, A. Osterloh, J. Siewert, and A. Uhlmann, New J. Phys. **10**, 043014 (2008).
[10] A. Osterloh, J. Siewert, and A. Uhlmann, Phys. Rev. A **77**, 032310 (2008).
[11] E. Jung, M.-R. Hwang, D. K. Park, and J.-W. Son, Phys. Rev. A **79**, 024306 (2009).
[12] H. Shu-Juan, W. Xiao-Hong, F. Shao-Ming, S. Hong-Xiang, and W. Qiao-Yan, Commun. Theor. Phys. **55**, 251 (2011).
[13] C. Eltschka and J. Siewert, Phys. Rev. Lett. **108**, 020502 (2012).
[14] J. Siewert and C. Eltschka, Phys. Rev. Lett. **108**, 230502 (2012).
[15] C. Eltschka and J. Siewert, Phys. Rev. A **89**, 022312 (2014).
[16] G. Sentís, C. Eltschka, and J. Siewert, Phys. Rev. A **94**, 020302(R) (2016).
[17] K. Cao, Z.-W. Zhou, G.-C. Guo, and L. He, Phys. Rev. A **81**, 034302 (2010).
[18] S. Rodriques, N. Datta, and P. Love, Phys. Rev. A **90**, 012340 (2014).
[19] A. Osterloh, Phys. Rev. A **93**, 052322 (2016).
[20] A. Osterloh, Phys. Rev. A **94**, 012323 (2016).
[21] E. Jung and D. Park, Phys. Rev. A **94**, 042330 (2016).
[22] V. Coffman, J. Kundu, and W. K. Wootters, Phys. Rev. A **61**, 052306 (2000).
[23] Y.-C. Ou and H. Fan, Phys. Rev. A **75**, 062308 (2007).
[24] H. He and G. Vidal, Phys. Rev. A **91**, 012339 (2015).
[25] B. Regula, S. Di Martino, S. Lee, and G. Adesso, Phys. Rev. Lett. **113**, 110501 (2014).
[26] B. Regula, S. Di Martino, S. Lee, and G. Adesso, Phys. Rev. Lett. **116**, 049902(E) (2016).
[27] B. Regula and G. Adesso, Phys. Rev. Lett. **116**, 070504 (2016).
[28] S. Karmakar, A. Sen, A. Bhar, and D. Sarkar, Phys. Rev. A **93**, 012327 (2016).
[29] A. Wong and N. Christensen, Phys. Rev. A **63**, 044301 (2001).
[30] F. Verstraete, J. Dehaene, and B. De Moor, Phys. Rev. A **68**, 012103 (2003).
[31] A. Osterloh and J. Siewert, Phys. Rev. A **72**, 012337 (2005).
[32] A. Cayley, J. Reine Angew. Math. **30**, 1 (1846).
[33] A. Miyake and M. Wadati, Quantum Inf. Comput. **2**, 540 (2002), arXiv:quant-ph/0212146.
[34] C. Eltschka, A. Osterloh, and J. Siewert, Phys. Rev. A **80**, 032313 (2009).
[35] B. Regula, A. Osterloh, and G. Adesso, Phys. Rev. A **93**, 052338 (2016).
[36] J.-G. Luque, J.-Y. Thibon, and F. Toumazet, Math. Struct. Comp. Sc. **17**, 1133 (2007), arXiv:quant-ph/0604202.
[37] M. Johansson, M. Ericsson, E. Sjöqvist, and A. Osterloh, Phys. Rev. A **89**, 012320 (2014).